
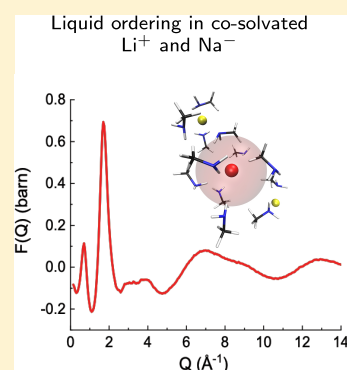


Solvation of Na^- in the Sodide Solution, $\text{LiNa}\cdot 10\text{MeNH}_2$ Andrew G. Seel,^{*,†,‡,§} Nicole Holzmann,[§] Silvia Imberti,^{||} Leonardo Bernasconi,^{⊥,||} Peter P. Edwards,[‡] Patrick L. Cullen,[†] Christopher A. Howard,^{†,||} and Neal T. Skipper^{†,||}[†]Department of Physics and Astronomy, University College London, Gower Street, London WC1E 6BT, U.K.[‡]Department of Chemistry, Inorganic Chemistry Laboratory, University of Oxford, South Parks Road, Oxford OX1 3QR, U.K.[§]Scientific Computing Department and ^{||}ISIS Facility, Rutherford Appleton Laboratory, Chilton, Didcot, Oxon OX11 0QX, U.K.[⊥]Center for Research Computing, University of Pittsburgh, 4420 Bayard Street, Pittsburgh, Pennsylvania 15260, United States Supporting Information

ABSTRACT: Alkalides, the alkali metals in their -1 oxidation state, represent some of the largest and most polarizable atomic species in condensed phases. This study determines the solvation environment around the sodide anion, Na^- , in a system of co-solvated Li^+ . We present isotopically varied total neutron scattering experiments alongside empirical potential structure refinement and ab initio molecular dynamics simulations for the alkali–alkalide system, $\text{LiNa}\cdot 10\text{MeNH}_2$. Both local coordination modes and the intermediate range liquid structure are determined, which demonstrate that distinct structural correlations between cation and anion in the liquid phase extend beyond 8.6 \AA . Indeed, the local solvation around Na^- is surprisingly well defined with strong solvent orientational order, in contrast to the classical description of alkalide anions not interacting with their environment. The ion-paired $\text{Li}(\text{MeNH}_2)_4^+\cdot\text{Na}^-$ species appears to be the dominant alkali–alkalide environment in these liquids, whereby Li^+ and Na^- share a MeNH_2 molecule through the amine group in their primary solvation spheres.

**INTRODUCTION**

The stability of group 1 metals in a formally negative oxidation state in polar solvents is rare, due to both the highly reducing nature of these alkalide anions or their being unstable with respect to dissociation to yield solvated cations and electrons such as in the case of metal–ammonia solutions.^{1,2} As such, the majority of alkalide systems are formed in nonpolar solvents via the dissolution of the alkali metal in the presence of a chelate, such as crown ether or cryptand.³ Their ns^2 electron configuration and notably large size have led to alkalides being labeled “gas-like” in nature in condensed phases, as first noted by their almost invariant chemical shifts in NMR measurements.^{4,5} The sodide anion, Na^- , exemplifies this particularly well, exhibiting a ^{23}Na NMR shift of around -63 ppm and linewidth of only a few hertz in a range of weakly polar solvents, seeming to indicate that it does not seem to interact to a significant extent with its local solvation environment. This noninteracting view has been challenged recently through ab initio calculations which suggest that although the anionic integrity of alkalides is maintained, close ion pairs with the encapsulated cation may be the prevailing species in nonpolar solvents, which may exhibit the same chemical shift and optical absorbance characteristics of the isolated alkalide.⁶ Furthermore, it is interesting to note that a crystalline alkalide with alkali–alkalide ion contacts still exhibits the same ^{23}Na NMR and optical absorbance as dilute sodides.⁷ Knowing the solvation and liquid structures of alkalide solutions would be of fundamental importance in our understanding of their properties, particularly in light of their

very high polarizabilities. Na^- , for example, is predicted to have a condensed-phase polarizability at least an order of magnitude higher than I^- ,^{8,9} which has led to the discussion of a potential insulator-to-metal transition under the Herzfeld criterion.¹⁰ This current study has been prompted by the lack of experimentally derived structural data for alkalide solutions, which are needed to guide calculations of their electronic properties or the critical concentration of alkalides, as we approach any metal-to-insulator transition.

The chemically most simple alkalide solution currently known is also quite the anomaly,¹¹ being formed by co-dissolution of lithium and sodium in liquid methylamine (MeNH_2) rather than a combination of nonpolar solvent and chelate. The ethylamine analogue is also known.¹² Although both metals are solvated by methylamine, the alkali metal cation (Li^+) and anion (Na^-) are formed rather than the alkali cation and solvated electron as in the case of the $\text{Li}-\text{MeNH}_2$ system (and indeed both $\text{Li}-\text{NH}_3$ and $\text{Na}-\text{NH}_3$).^{13–15} The $\text{LiNa}\cdot n\text{MeNH}_2$ system shares many similarities to the metal–ammonia and metal–amine liquids, despite containing a genuine alkalide species as opposed to solvated electrons. It can be formed up to an extremely high metal concentration and exhibits a transition from the electrolytic alkalide solution to a metallic state at high concentrations, accompanied by a smooth deshielding of the Na^- chemical shift.¹¹ This transition

Received: April 23, 2019

Revised: May 30, 2019

Published: May 30, 2019

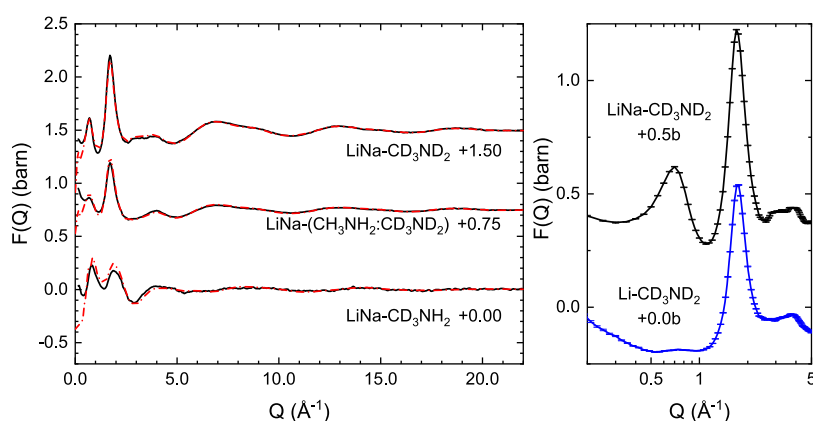


Figure 1. Left: $F(Q)$ data for isotopically unique samples of LiNa-10MeNH₂. From top to bottom: CD₃NH₂, CD₃ND₂, CH₃NH₂:CD₃ND₂, 2CH₃NH₃:CD₃ND₂. Data are offset by the given amount for clarity, and EPSR refinements to the data are shown by the dashed red line. Right: $F(Q)$ for LiNa-10MeND₂ (above) and Li(e⁻)·10MeND₂ (below).

from an insulating Li⁺Na⁻ solution to metallic liquid occurs for $n < 6$ in LiNa- n MeNH₂, and the concentration limit is believed to be as high as $n = 3$.

To understand the structural relationship and hence the stability of Na⁻ in the presence of solvated Li⁺, this study details the structure of the LiNa–MeNH₂ system in the liquid electrolyte phase. We are able to use combined experimental and modeling techniques to determine the solvation structure around each metal species, in addition to longer-range correlations between alkali and alkali.

EXPERIMENTAL DETAILS

Na metal is not soluble in MeNH₂ but does dissolve in Li(MeNH₂)_{*x*}. As such, each isotopically unique sample for this work was prepared in an identical fashion following the procedures of Dye et al.¹¹ Initially, stoichiometric amounts of clean Li and Na metal were co-dissolved in anhydrous NH₃ within quartz tubes of 4 mm internal diameter. The NH₃ was then slowly distilled to leave a mirror of finely divided Li/Na. The metal was then maintained under a vacuum <10⁻⁶ mbar for a period of approximately 20 h to ensure that all NH₃ had been removed before anhydrous MeNH₂ was condensed onto the metal. The sample was allowed to equilibrate at 200 K for a period of 6 h before being frozen in liquid nitrogen and the quartz tube being flame-sealed. The samples were never exposed to temperatures above 200 K, and no decomposition was detected throughout the process, in line with the findings of Dye et al.

Neutron scattering measurements were performed using the SANDALS instrument at the ISIS Spallation Neutron and Muon Source, U.K. Each sealed sample was contained within a thin vanadium sheath to be suspended in the beam, before being equilibrated and measured at 210 K until a minimum of 600 μAh proton current counts. As with previous studies of the liquid structure of metal amines, all empty containers, sheaths, and instrument background measurements were collected, and the sample data corrected for this sample containment, multiple scattering, and incoherent corrections using the standard procedures for total scattering data.^{16–19} The resulting scattering function is of the form:

$$F(Q) = \sum_{\alpha=1}^n \sum_{\beta=1}^n c_{\alpha} c_{\beta} b_{\alpha} b_{\beta} [S_{\alpha\beta}(Q) - 1] \quad (1)$$

where $S_{\alpha\beta}(Q)$ is the Faber–Ziman partial structure factor, c_{α} and b_{α} the atomic fraction and neutron coherent scattering length of atom α , respectively. $S_{\alpha\beta}(Q)$ is the Fourier transform of the real-space pair distribution functions, $g_{\alpha\beta}(r)$.

Structural models for the liquid system were refined to each unique neutron dataset simultaneously using the empirical potential structure refinement (EPSR) software.²⁰ The exact density of the alkali solutions is not known but was estimated from the work of Pyper and Edwards to be 0.09275 atoms Å⁻³.⁸ This value was consistent with the total measured neutron scattering power of the samples. The EPSR method is detailed elsewhere²⁰ and requires seed Lennard-Jones and Coulomb potentials prior to the refinement of both the empirical potential and structural model. Input Lennard-Jones potentials for methylamine were taken from Jorgensen et al.²¹ The simulation box contained 500 formula units of the system, equivalent to 6000 molecules. During the initial structural relaxation of a randomized simulation box, it was required to constrain the Na–Na approaches to have a lower bound value of 6.0 Å. Once the system had reached an initial convergence, this constraint was removed and the system allowed to evolve freely.

For ab initio molecular dynamics (AIMD) simulations, the geometry of tetrahedrally coordinated [Li(MeNH₂)₄]⁺ was initially optimized applying density functional theory (DFT) at the B3LYP^{22,23}/def2-TZVPP²⁴ level of theory with the NWChem6.6 program package.²⁵ The full simulation box was formed by taking eight units of the latter and arranging them in a cubic fashion with a Li–Li distance of 9.2 Å. Eight sodium ions were placed offset to lithium so that the Li and Na atoms correspond to a cubic unit cell. The remaining 48 MeNH₂ molecules were randomly placed within the box dimensions with the program packmol.²⁶ AIMD simulations and preceding optimization steps were then performed using the hybrid Gaussian/plane-wave²⁷ package CP2K Quickstep^{28,29} version 3.0. The PBE functional,^{30–32} standard double- ζ VB basis sets and Goedecker–Teter–Hutter pseudopotentials³³ were used for all atomic species. A cutoff of 310 Ry was used in the plane-wave expansion. Preoptimization steps (200) were carried out prior to simulation. Atomic positions were then propagated using the Born–Oppenheimer dynamics³⁴ in an NVT ensemble and with a time-step of 0.5 fs under periodic boundary conditions. For the first 2 ps, the positions of sodium and the

$[\text{Li}(\text{MeNH}_2)_4]^+$ units were held fixed, following 8 ps of fully relaxed simulation. The simulation temperature was set to 500 K and was controlled through a Nosé–Hoover thermostat. The implementation of dispersion correction at the DFT-D3 level³⁵ was not found to affect our results to any notable degree and is included in the Supporting Information. Visualization of results and $g(r)$ analyses were done using visual molecular dynamics (VMD).³⁶ Trajectory data after a 0.5 ps equilibration period of the fully relaxed simulation was considered for analysis.

RESULTS AND DISCUSSION

The total neutron scattering functions for the isotopically unique liquid samples are presented in Figure 1. As can be immediately seen, there exists a prepeak in the data at 0.73 \AA^{-1} . This prepeak corresponds to a real-space intermediate range order of 8.6 \AA and can be assigned to probable cation–cation or anion–anion distances. It is interesting to note that only concentrated, metallic Li– NH_3 and Li– MeNH_2 solutions exhibit this prepeak,^{16,18} but the dilute, solvated electron systems do not. Indeed, the sodide anion is the same approximate volume as that occupied by a solvated electron in dilute metal–amine solutions ($\sim 5 \text{ \AA}$ diameter), yet comparing the neutron scattering spectra of $\text{Li}^+\text{Na}^- \cdot 10\text{MeNH}_2$ and $\text{Li}^+\text{e}^- \cdot 10\text{MeNH}_2$, we see that the sodide templates the long-ranged liquid structure to a far greater extent than does the solvated electron. Intuition may posit that the local structure around the sodide is likewise more ordered, which indeed this study will show.

Included in Figure 1 are the EPSR fits to the data, and it can be seen that the agreement with the neutron scattering data is good for all samples. The intensity mismatch at the lowest Q values corresponds to correlations far beyond intermediate range ordering and arises due to both finite size effects from the EPSR simulation box and from the difficulty of removing all incoherent and multiple scattering intensities due to the cylindrical geometry of the sample cells.

Li- and Na-centered atom–atom pair distribution functions extracted from the EPSR model of the neutron data are presented in Figure 2. The lithium environment is consistent with that found for Li– MeNH_2 liquids in both the electrolytic and metallic phases, and found in gas-phase investigations, being tetra-coordinate about the cation through the amine nitrogen. The most probable Li–N distance is found to be 2.09 \AA , with a LiNC angle of 102.5° drawing the methyl groups toward the metal to some extent while still notably lying beyond the coordinating amine component. Na^- is found to be solvated on average by 8 methylamine molecules. The nearest-atom approach is by the amine protons at 3.3 \AA , with the methyl protons lying on average 0.5 \AA further out from the sodide. Both exhibit a notable structure in their extracted $g_{\text{NaX}}(r)$, which is also the case for Na–N and Na–C pairs, possessing primary solvation distances to the sodide of 4.2 and 4.8 \AA , respectively. As such we can state that the solvation structure around Na^- is distinctly ordered, and that although the dominant solvation of sodide is primarily through the amine protons, the N–C axis of methylamine is drawn toward the anion surface providing additional solvation contributions from methyl protons. Figure 3 depicts isosurfaces extracted from the neutron-fitted EPSR refinement for the distribution of Na^- and Li^+ around a methylamine molecule. It is interesting to also consider the extracted $g_{\text{LiNa}}(r)$, which exhibits a principal maximum at 5.2 \AA . This is consistent with Na^-

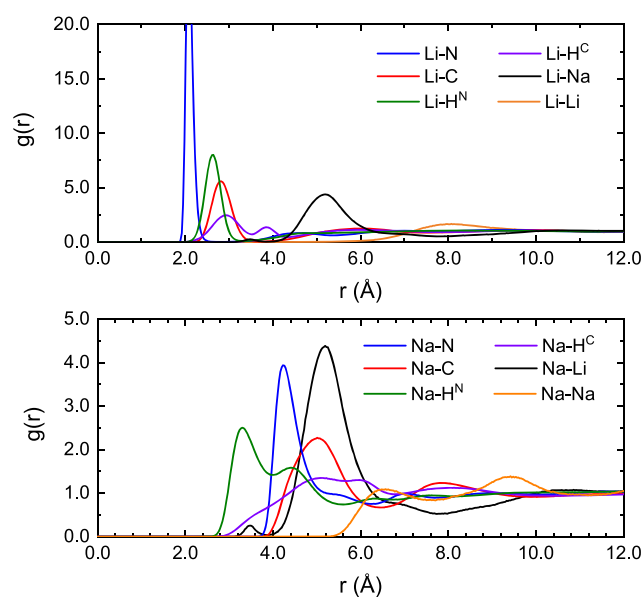


Figure 2. Li^+ - (top) and Na^- -centered (bottom) partial pair distribution functions from the EPSR model refinement. Note the differing ordinate scales.

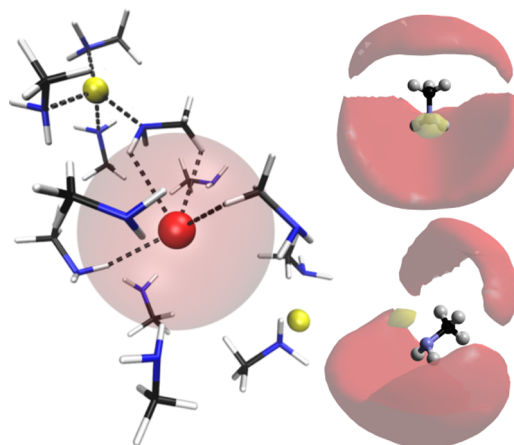


Figure 3. Left: AIMD snapshot for the coordination of methylamine around Li^+ (yellow) and Na^- (red) showing distinct coordination modes. Right: EPSR-derived spatial density plots for the distribution of Li and Na around MeNH_2 , 0.6 probability isosurface shown.

sharing a primary solvation sphere with Li^+ through the amine protons of the $[\text{Li}(\text{MeNH}_2)_4]^+$ complex. This solvent-mediated ion pairing contributes to the intermediate range ordering of the liquid sodide on the insulating side of the metal-to-insulator transition, where we may consider the system to be an almost negligibly solvated ionic liquid of Na^- and $\text{Li}(\text{MeNH}_2)_4^+$.

Although the EPSR model refines both structure and atom pair potentials to the neutron scattering data, the description of intermolecular interactions as Lennard-Jones, Coulombic, and empirical potential terms is still a relatively crude description, particularly of Na^- . To further validate our structural model, we can compare it with AIMD simulation. As opposed to the hardness of the neutron-refined model, the density functional used in the AIMD simulations should overpolarize or underbind the electron density in dilute systems such as Na^- . The AIMD data presented stem from an analyzed trajectory of an 8:8:80 Li/Na/ MeNH_2 system with a post-

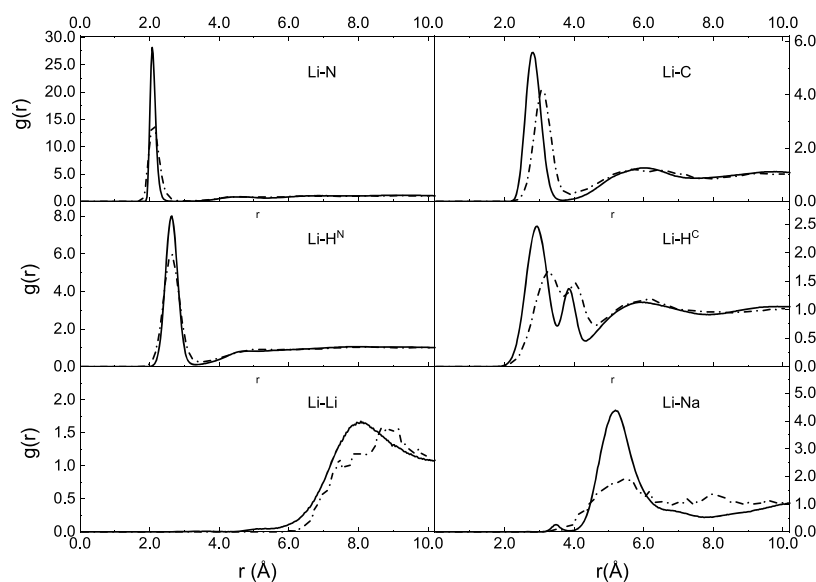


Figure 4. Comparison between EPSR- (continuous line) and AIMD (dashed line)-derived pair distribution functions $g_{\text{LiX}}(r)$.

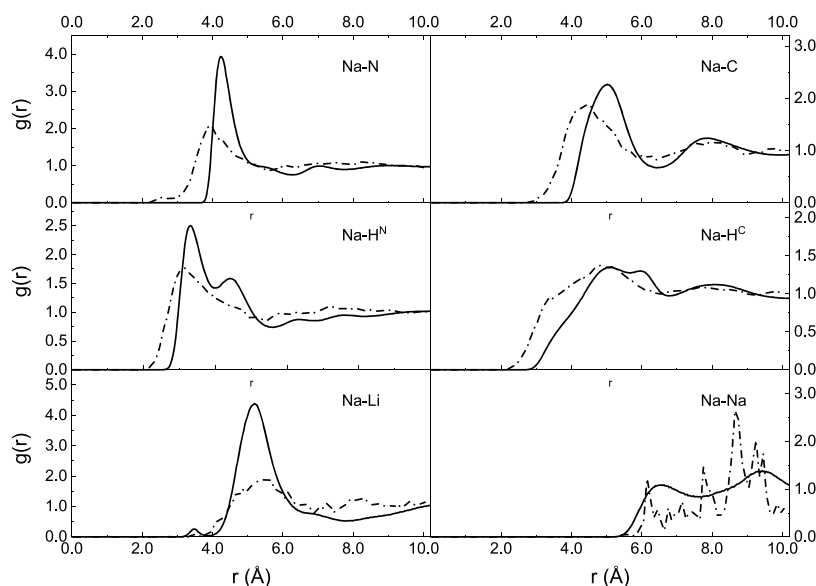


Figure 5. Comparison between EPSR- (continuous line) and AIMD (dashed line)-derived pair distribution functions $g_{\text{NaX}}(r)$.

relaxation duration of 7.5 ps. As an artefact in the simulation, we observed one pair of sodide ions aggregating and oscillating at a distance between 3 and 4.8 Å and have not included this in our subsequent analyses. As expected in the electronic structure for the system, the eight highest occupied orbitals (HOMO to HOMO-7) correspond to Na-centered orbitals of s-symmetry, confirming the anionic nature of this atom. Interestingly, in crystalline phases of alkali salts, the calculated electron density around the alkali is not always spherically symmetric, but this seems to be limited to heavier alkalis than Na^- and influenced by the neighboring alkali cation complexes.³⁷ Certainly, the solvation around the alkali plays a role in its electronic structure. Our results for $g_{\text{LiX}}(r)$ and $g_{\text{NaX}}(r)$ extracted from AIMD and EPSR are presented in Figures 4 and 5. We find a general trend of the AIMD simulation fitting well the nearest atom-atom approaches for both Li^+ and Na^- through the amine nitrogen and proton, respectively, but with increasing disparity as we venture away

from either metal center. Compared to our empirical potential model, we find that solvation numbers are consistent but that AIMD derived peaks in $g(r)$ are broader, reflecting the tendency for density functional methods to underbind solvation structures. This is most noticeable for the cases of $g_{\text{NaX}}(r)$ where resolved undulations in the EPSR model are broadened in the AIMD case, and the amine protons are drawn 0.2 Å closer to the sodide than in the EPSR model.

Nevertheless, the agreement in the primary solvation environment of Li^+ and Na^- in our two structural models allows us to describe the manner in which methylamine is able to co-solvate this alkali-alkali system. Clearly, a dominant role is played by the amine group in both cation and anion solvation, as shown in Figure 3. In addition to coordination modes from the amine protons alone, the AIMD trajectory data also show solvation structures whereby one or two amine and methyl protons are coordinated to the sodide. This corresponds to the additional role of methyl protons around

Na^- resulting from our experimentally derived EPSR calculations. In both cases, we observe the respective methylamine nitrogen atom also coordinating to Li^+ , contributing to the definition of Li within the immediate solvation structure of sodide. The shared amine solvation with Li^+ and methyl protons helps us to understand how such a diffuse, reducing species as Na^- is able to maintain its anionic nature in the presence of a confining potential produced by so few solvent molecules and indeed not in the presence of ammonia as opposed to methylamine.

CONCLUSIONS

We have used isotopically varied neutron scattering data, coupled to empirical potential structure refinements and ab initio molecular dynamics simulation, to investigate the solvation structure of Li^+ and Na^- in methylamine solution. This concentrated alkali solution reveals a shared primary solvation between alkali and alkalide and has allowed us to categorize the solvation of a sodide anion as primarily being through both amine and methyl protons in solution. Clearly, even this weak confining potential is able to generate the sodide in the presence of close, coordinated alkali cations. Previous studies have suggested that even slight concentration of this system takes it to the very verge of metallization, which we may consider as being prevented by the preferred orientation of the amine solvent between alkali and alkalide. We have yet to determine how the environment of sodide changes as we further approach this limit, by either a further concentration of alkali–alkalide or the application of external pressure. These present a challenge both experimentally and computationally due to the high polarizability and diffuse nature of Na^- . Clearly the role of the solvent must change, but whether we first enter a system of solvent-mediated $\text{Li}^{\delta+}\text{Na}^{\delta-}$ or a sudden structural transition accompanies metallization is still to be determined.

Finally, we note that this study suggests that sodide systems are more ordered in the liquid phase than the equivalent solvated electron systems of the same concentration. This is demonstrated by a distinct prepeak in our sodide neutron scattering spectra, which is witnessed in metallic metal–amine solutions that are known to form crystalline compounds in their concentration limit (the expanded metals $\text{Li}(\text{NH}_3)_4$, $\text{Ca}(\text{NH}_3)_6$, $\text{Li}(\text{MeNH}_2)_4$ and, as of this study, the suggested $\text{LiNa}(\text{MeNH}_2)_{3,4}$).^{16,18,38} Interestingly, it is increasingly being realized that such a prepeak is extremely weak or absent for systems, which do not form solid compounds ($\text{Na}-\text{NH}_3$, $\text{K}-\text{NH}_3$).^{17,39} Concerning the possibility of synthesizing new expanded metals: were we to try and extend their number into crystalline phases comprising mixed-metal or mixed-solvent systems, we may suggest that such a feat be linked to the existence of structuring in the solution phase.

ASSOCIATED CONTENT

Supporting Information

The Supporting Information is available free of charge on the ACS Publications website at DOI: 10.1021/acs.jpcc.9b03792.

DFT-D3: A comparison between calculated $g_{\text{LiX}}(r)$ and $g_{\text{NaX}}(r)$ with (red line) and without (black line) dispersion correction (PDF)

AUTHOR INFORMATION

Corresponding Author

*E-mail: a.seel@ucl.ac.uk.

ORCID

Andrew G. Seel: 0000-0003-0103-8388

Silvia Imberti: 0000-0001-7037-6829

Leonardo Bernasconi: 0000-0002-9460-7975

Christopher A. Howard: 0000-0003-2550-0012

Neal T. Skipper: 0000-0003-2940-3084

Notes

The authors declare no competing financial interest.

ACKNOWLEDGMENTS

We would like to thank the ISIS facility and STFC for the use of SANDALS and allocation of beamtime RB1720402, Dr Sabrina Gaertner and Damian Fornalski for their aid in the experiment. We would also like to thank Prof. Keith Refson for stimulating discussion. A.G.S., C.A.H., and N.T.S. thank the Leverhulme trust for funding. P.L.C. thanks the EPSRC for funding under fellowship EP/S001298/1. N.H. and L.B. thank the Materials Chemistry Consortium for access to the ARCHER U.K. Supercomputing Service funded by the EPSRC (EP/L000202) and the STFC for access to the SCARF cluster.

REFERENCES

- (1) Dye, J. L. The alkali metals: 200 years of surprises. *Philos. Trans. R. Soc., A* **2017**, *373*, No. 0174.
- (2) Lok, M. T.; Tehan, F. J.; Dye, J. L. Spectra of Na-, K-, and e- solv in amines and ethers. *J. Phys. Chem.* **1972**, *76*, 2975–2981.
- (3) Dye, J. L.; Redko, M. Y.; Huang, R. H.; Jackson, J. E. Role of cation complexants in the synthesis of alkalides and electrides. *Adv. Inorg. Chem.* **2006**, *59*, 205–231.
- (4) Edwards, P. P. Nuclear magnetic resonance studies of alkali metals in nonaqueous solvents. *J. Phys. Chem.* **1984**, *88*, 3772–3780.
- (5) Pyper, N. C.; Edwards, P. P. Nuclear shielding in the alkali metal anions. *J. Am. Chem. Soc.* **1986**, *108*, 78–81.
- (6) Zurek, E. Alkali metals in ethylenediamine: A computational study of the optical absorption spectra and NMR parameters of $[\text{M}(\text{en})_3^{\delta+}\cdot\text{M}^{\delta-}]$ ion pairs. *J. Am. Chem. Soc.* **2011**, *133*, 4829–4839.
- (7) Kuchenmeister, M. E.; Dye, J. L. Synthesis and structures of two thermally stable sodides with the macrocyclic complexant hexamethyl hexacyclen. *J. Am. Chem. Soc.* **1989**, *111*, 935–938.
- (8) Pyper, N. C.; Edwards, P. P. Metallization of alkali anions in condensed phases. *J. Am. Chem. Soc.* **2000**, *122*, 5092–5099.
- (9) Glover, W. J.; Larsen, R. E.; Schwartz, B. J. The roles of electronic exchange and correlation in charge-transfer-to-solvent dynamics: Many-electron nonadiabatic mixed quantum/classical simulations of photoexcited sodium anions in the condensed phase. *J. Chem. Phys.* **2008**, *129*, No. 164505.
- (10) Herzfeld, K. F. On Atomic Properties which make an Element a Metal. *Phys. Rev.* **1927**, *29*, 701.
- (11) DeBacker, M. G.; Mkadmi, E. B.; Sauvage, F. X.; Lelieur, J. P.; Wagner, M. J.; Concepcion, R.; Kim, J.; McMills, L. E. H.; Dye, J. L. The lithium-sodium-methylamine system: Does a low-melting sodide become a liquid metal? *J. Am. Chem. Soc.* **1996**, *118*, 1997–2003.
- (12) DeBacker, M. G.; Mkadmi, E. B.; Sauvage, F. X.; Lelieur, J. P.; Wagner, M. J.; Concepcion, R.; Elgin, J. L.; Guadagnini, R. A.; Kim, J.; McMills, L. E. H.; Dye, J. L. Lithium-Ethylamine and Lithium-Sodium-Ethylamine Systems: A Nonmetallic Liquid Electride and the Lowest Melting Fused Salt. *J. Am. Chem. Soc.* **1994**, *116*, 6570–6576.
- (13) Zurek, E.; Edwards, P. P.; Hoffmann, R. A molecular perspective on lithium-ammonia solutions. *Angew. Chem., Int. Ed.* **2009**, *48*, 8198–8232.

- (14) Edwards, P. P.; Buntaine, J. R.; Sienko, M. J. Electron- and nuclear-spin-lattice relaxation and the metal-nonmetal transition in lithium-methylamine solutions. *Phys. Rev. B* **1979**, *19*, 5835–5846.
- (15) Thompson, J. C. *Electrons in Liquid Ammonia*; Oxford University Press, 2009.
- (16) Thompson, H.; Wasse, J. C.; Skipper, N. T.; Hayama, S.; Bowron, D. T.; Soper, A. K. Structural studies of ammonia and metallic lithium-ammonia solutions. *J. Am. Chem. Soc.* **2003**, *125*, 2572–2581.
- (17) Wasse, J. C.; Hayama, S.; Masmanidis, S.; Stebbings, S. L.; Skipper, N. T. The structure lithium-ammonia and sodium-ammonia solutions by neutron diffraction. *J. Chem. Phys.* **2003**, *118*, No. 7486.
- (18) Hayama, S.; Wasse, J. C.; Soper, A. K.; Skipper, N. T. The structure of solutions of lithium in methylamine across the metal-nonmetal transition. *J. Phys. Chem. B* **2002**, *106*, 11–14.
- (19) Seel, A. G.; Swan, H.; Bowron, D. T.; Wasse, J. C.; Weller, T.; Edwards, P. P.; Howard, C. A.; Skipper, N. T. Electron solvation and the unique liquid structure of a mixed-amine expanded metal: The saturated Li-NH₃-MeNH₂ system. *Angew. Chem., Int. Ed.* **2017**, *56*, 1561–1565.
- (20) Soper, A. K. Partial structure factors from disordered materials diffraction data: An approach using empirical potential structure refinement. *Phys. Rev. B* **2005**, *72*, No. 104204.
- (21) Rizzo, R. C.; Jorgensen, W. L. OPLS All-Atom Model for Amines: Resolution of the Amine Hydration Problem. *J. Am. Chem. Soc.* **1999**, *121*, 4827–4836.
- (22) Becke, A. D. Density-functional thermochemistry. iii. the role of exact exchange. *J. Chem. Phys.* **1993**, *98*, 5648–5652.
- (23) Lee, C.; Yang, W.; Parr, R. G. Development of the colle-salvetti correlation-energy formula into a functional of the electron density. *Phys. Rev. B* **1988**, *37*, 785–789.
- (24) Weigend, F.; Ahlrichs, R. Balanced basis sets of split valence, triple zeta valence and quadruple zeta valence quality for H to Rn: Design and assessment of accuracy. *Phys. Chem. Chem. Phys.* **2005**, *7*, 3297–3305.
- (25) Valiev, M.; Bylaska, E. J.; Govind, N.; Kowalski, K.; Straatsma, T. P.; van Dam, H. J. J.; Wang, D.; Nieplocha, J.; Apra, E.; Windus, T. L.; de Jong, W. A. A comprehensive and scalable open-source solution for large scale molecular simulations. *Comput. Phys. Commun.* **2010**, *181*, 1477–1489.
- (26) Martínez, L.; Andrade, R.; Birgin, E. G.; Martínez, J. M. A package for building initial configurations for molecular dynamics simulations. *J. Comput. Chem.* **2009**, *30*, 2157–2164.
- (27) Lippert, B. G.; Hutter, J.; Parrinello, M. A hybrid gaussian and plane wave density functional scheme. *Mol. Phys.* **1997**, *92*, 477–488.
- (28) van de Vondele, J.; Krack, M.; Mohamad, F.; Parrinello, M.; Chassaing, T.; Hutter, J. Quickstep: Fast and accurate density functional calculations using a mixed gaussian and plane waves approach. *Comput. Phys. Commun.* **2005**, *167*, 103–128.
- (29) <https://www.cp2k.org/quickstep>.
- (30) Slater, J. C. A simplification of the hartree-fock method. *Phys. Rev.* **1951**, *81*, 385–390.
- (31) Perdew, J. P.; Wang, Y. Accurate and simple analytic representation of the electron-gas correlation energy. *Phys. Rev. B* **1992**, *45*, 13244–13249.
- (32) Perdew, J. P.; Burke, K.; Ernzerhof, M. Generalized gradient approximation made simple. *Phys. Rev. Lett.* **1996**, *77*, 3865–3868.
- (33) Goedecker, S.; Teter, M.; Hutter, J. Separable dual-space gaussian pseudopotentials. *Phys. Rev. B* **1996**, *54*, 1703–1710.
- (34) Grotendorst, J. *Modern Methods and Algorithms of Quantum Chemistry*; NIC-Directors, 2000.
- (35) Grimme, S.; Antony, J.; Ehrlich, S.; Krieg, H. A consistent and accurate *ab initio* parametrization of density functional dispersion correction (DFT-D) for the 94 elements H-Pu. *J. Chem. Phys.* **2010**, *132*, No. 154104.
- (36) Humphrey, W.; Dalke, A.; Schultern, K. Vmd: Visual molecular dynamics. *J. Mol. Graphics Modell.* **1996**, *14*, 33–38.
- (37) Dale, S. G.; Becke, A. D.; Johnson, E. R. Density-functional description of alkalides: introducing the alkalide state. *Phys. Chem. Chem. Phys.* **2018**, *20*, 26710.
- (38) Wasse, J. C.; Howard, C. A.; Thompson, H.; Skipper, N. T.; Delaplane, R. G.; Wannberg, A. The structure of calcium-ammonia solutions by neutron diffraction. *J. Chem. Phys.* **2004**, *121*, 996.
- (39) Wasse, J. C.; Hayama, S.; Skipper, N. T.; Benmore, C. J.; Soper, A. K. The structure of saturated lithium- and potassium-ammonia solutions as studied by neutron diffraction. *J. Chem. Phys.* **2000**, *112*, 7147–7151.